13th IEA Heat Pump Conference
April 26-29, 2021 Jeju, Korea

High-temperature vapor compression heat pump using butane (R600) – development of a prototype and first measurements

Manuel Verdnik[a,*], René Rieberer[a]

[a]Graz University of Technology, Institute of Thermal Engineering, Inffeldgasse 25B, 8010 Graz, Austria

Abstract

The application of industrial heat pumps for waste heat recovery can reduce the usage of fossil fuels and increase the energy efficiency of industrial processes. Utilizing a trans-critical vapor compression cycle extends the operating range of refrigerants beyond their critical temperature, enabling high heat sink temperatures with natural refrigerants, which are characterized by zero ozone depletion potential and a negligible global warming potential.
To prove the concept of a trans-critical vapor compression cycle using butane as refrigerant, a prototype to achieve a nominal heating capacity of 30 kW at heat sink outlet temperatures of up to 160 °C for utilizing waste heat (at 60 °C) was developed. The one-stage cycle with a suction gas cooled reciprocating compressor is equipped with a low-pressure accumulator and an internal heat exchanger (IHX) for suction gas superheating. First measurements of sub-critical and trans-critical operation show remarkable coefficients of performance (COPs) and confirm that optimum high-side pressures yielding the maximum COP exist. In trans-critical operation the optimum pressure can be shifted towards lower pressures by increasing the suction gas superheat in the IHX.

Keywords: industrial heat pump; high-temperature application; hydrocarbons; optimum high-side pressure; trans-critical cycle;

Nomenclature

1…9	state point	p_{hp}	high-side pressure (bar)
accu	low-pressure accumulator	$\pi = p_{ref,1}/p_{ref,2}$	pressure ratio of the compressor (-)
COP	Coefficient of Performance	$\dot{Q}_{SI}$	heating capacity on water side (kW)
$\eta_{is,ov}$	overall isentropic efficiency (-)	ref	refrigerant
$\eta_{is,i}$	internal isentropic efficiency (-)	ρ	density (kg·m³)
η_{FI}	frequency inverter efficiency (-)	s	isentropic change of state
EXV	electric expansion valve	sat	saturated state
h	specific enthalpy (kJ/kg)	SI	heat sink
IHX	internal heat exchanger	sim	simulated
in	inlet	SO	heat source
λ_{vol}	volumetric efficiency	ΔT_{sup}	suction gas superheat (K)
meas	measured	t	temperature (°C)
$\dot{m}_{ref}$	refrigerant mass flow (kg/h)	t_{cond}	condensation temperature (°C)
out	outlet	$\dot{V}$	volume flow
p	absolute pressure (bar)	VIHX	3-way-valve internal heat exchanger
P_{el}	electric power of compressor and inverter (kW)	$\dot{V}_{swept}$	compressor swept volume flow (m³/h)

* Corresponding author. Tel.:+43 316 873-7304; fax: +43 316 873-7305.
E-mail address: manuel.verdnik@tugraz.at.

1. Introduction

Improving the efficiency of energy systems is a key to decrease energy consumption. Implementing all available energy efficiency measures between now and 2040 would allow to double the global gross domestic product by 2040 while limiting the increase in primary energy demand to levels only slightly higher than those today [1]. Through the application of high-temperature heat pumps, the utilization of waste heat to cover industrial process heat demands can be accomplished. A trans-critical vapor compression cycle as proposed by Lorentzen [2] offers the possibility to extend the operating range of refrigerants beyond their critical temperature. While this process is state-of-the art for CO_2, the application of other refrigerants is very limited. Besbes et al. [3] developed a high temperature trans-critical heat pump utilizing R32, capable of producing hot air at 120 °C. Abi Chahla et al. [4] extended the supply temperature to 150 °C by using the HFO 1234ze(E). Regarding natural refrigerants Kimura et al. [5] developed a test apparatus of a trans-critical cycle for R600 using oil-free turbocompressors enabling heat supply temperatures of 180 °C according to simulations.

This work is based on the development of a prototype of a vapor compression heat pump utilizing a natural refrigerant in a trans-critical cycle enabling heat supply temperatures higher than 150 °C. In a trans-critical cycle, the refrigerant is compressed to a supercritical state and the heat rejection occurs at high-side pressure levels exceeding the critical pressure of the refrigerant at gliding temperature. Considering the available components with respect to the necessary pressure, R600 was chosen as refrigerant. The influence of the operating parameters on the efficiency of the prototype were investigated by means of simulation. Measurement data of the prototype is compared to results from the simulation model. The prototype, simulation model and results from experiment and simulation as presented by Verdnik et al. [6] are analyzed in more detail and used to derive an improved simulation model.

2. Prototype of the trans-critical vapor compression heat pump

The development of the prototype was based on a study by Verdnik et al. [7] on the application of R600 in a trans-critical vapor compression cycle. The application specific challenges such as the required suction gas superheat due to the overhanging two phase region of the refrigerant and safety measures due to the flammability of the refrigerant were addressed during the design of the prototype.

2.1. Hydraulic layout

Fig. 1. shows the realized hydraulic layout and a picture of the prototype.

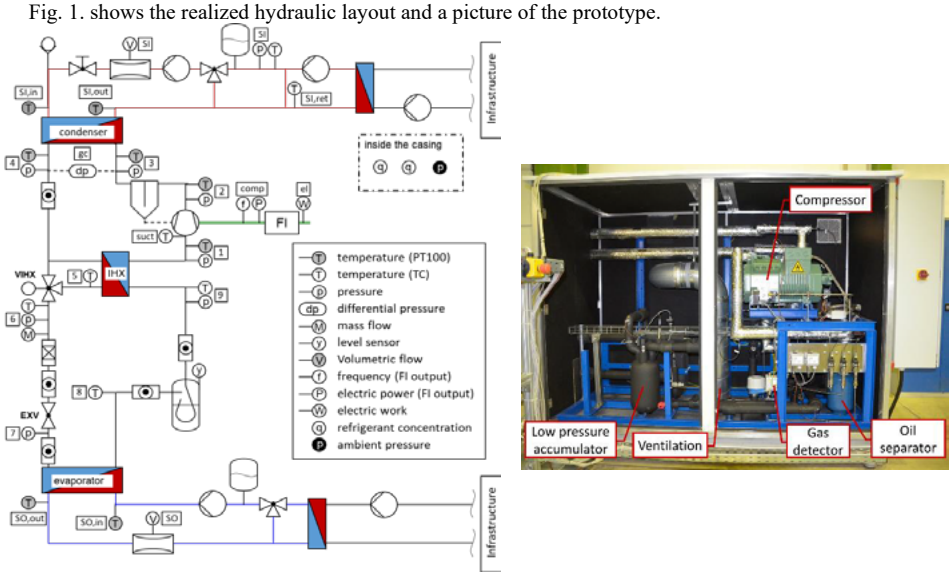

Fig. 1. Hydraulic layout including sensor positions of the high-temperature heat pump (left) and the prototype with opened casing (right)

The single stage cycle utilizes an inverter driven suction gas cooled reciprocating compressor. In order to maximize the evaporation temperature and to accomplish the necessary suction gas superheating in the internal heat exchanger (IHX) saturated refrigerant at the evaporator outlet is targeted. This is accomplished by using a low-pressure accumulator (accu) and the corresponding refrigerant charge to allow for a liquid level in the accumulator.

Experimental data from the prototype is shown in t/h-diagrams with operating points in sub-critical (Fig. 2 left) and trans-critical operation Fig. 2 (right). The state points are corresponding to Fig. 1.

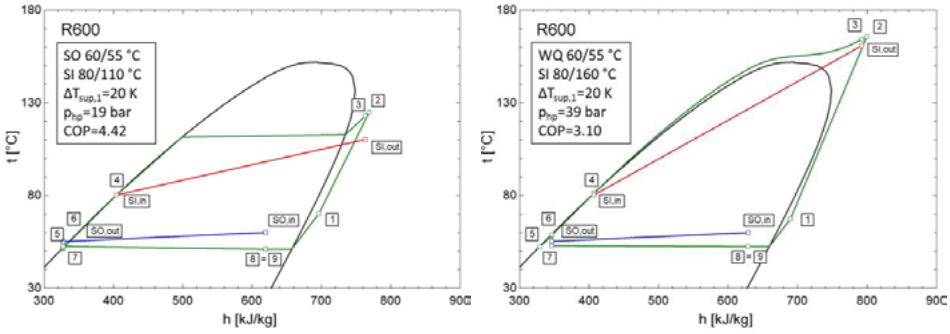

Fig. 2. t/h-diagrams of a measured sub-critical operating point (left) and trans-critical cycle operating point (right)

Refrigerants with an “overhanging” two phase region require a certain degree of suction gas superheat in order to avoid a compression into the two-phase region. According to Moisi and Rieberer [8], the required suction gas superheat for R600 is 18 K assuming a positive evaporation temperature and isentropic compression. At the prototype, the suction gas superheat is evaluated at the compressor suction port as well as before the refrigerant flows into the cylinder after cooling the electric motor according to equation (1) and (2), respectively. While the superheat before the cylinder acts as a threshold for the minimum superheat, the value at the control inlet is used as the control variable for the VIHX.

$$\Delta T_{sup,1} = t_{ref,1} - t_{sat}(p_{ref,1}) \tag{1}$$

$$\Delta T_{sup,suct} = t_{ref,suct} - t_{sat}(p_{ref,1}) \tag{2}$$

The three-way-valve (VIHX) controls the degree of suction gas superheat at state point 1. The electronic expansion valve (EXV) is used to control the high-side pressure. Assuring saturated vapor at the outlet of the evaporator and inlet of the IHX by using an accumulator also decouples the control loops for high-side pressure and suction gas superheat. In order to keep the pressure throughout the condenser above the set pressure and to dampen pressure oscillations from the compressor the condenser outlet pressure is used as the control variable for the high-side pressure control loop.

The auxiliary hydraulic cycles representing the heat source and heat sink use pressurized water at 10 bars which is corresponding to a boiling point of 180 °C. A hydraulic separator with a bypass pump is used in the sink cycle to avoid high return temperatures ($t_{SI,ret}$) at the heat exchanger connecting the test rig with the infrastructure.

Due to the flammability of the refrigerant, two gas detectors are installed in the machine casing. If the concentration of R600 reaches 20% of the lower flame level, an explosion proof ventilation system is activated and the power supply to the rest of the prototype is cut.

With exemption of the prototype compressor, off-the-shelf parts as listed in Table 1 are used in the trans-critical heat pump.

Table 1. Main components used in the refrigerant cycle

Component	Manufacturer	Specifications
Compressor	Bitzer	$\dot{V}_{swept}$ @50Hz 34.7 m³/h
Oil separator	ESK Schultze	V=7.5 l
VIHX	Siemens	p_{max}=43 bar
EXV	Carel	t_{max}=70 °C
Accumulator	Frigomec	V=7.8 l
Heat exchangers	Alfa Laval	Brazed plate with asymmetric channels
		Brazed plate
		Brazed plate

2.2. Measurement equipment and evaluation

The used measurement equipment is listed in Table 2 including the expected uncertainties of reading at the measured operating points of the prototype. The accuracy of the temperature sensors was determined through calibration. For the other measured quantities manufacturers' specifications regarding the accuracy of the sensor as well as the acquisition system were taken into consideration. The uncertainty of measurement of evaluated quantities have been estimated using the Gaussian Error Propagation implemented in the Engineering Equation Solver (EES) [9]. Properties of R600 and water are evaluated with EES.

Table 2. Measurement equipment used for evaluating the capacities and evaporation temperature

Measured quantity	Location	Sensor	Uncertainty of reading
Temperature	SI,in; SI,out	Pt100	± 0.1 K
Volumetric flow rate	SI	Electromagnetic flow meter	± 0.0015 l/s
Electric power consumption	el	Wattmeter	± 1% of reading
Pressure	4	Strain-Gauge	± 0.25 bar
Pressure	7	Strain-Gauge	± 0.09 bar

The systems COP is evaluated according to equation (3) by averaging 10 minute long measurements of steady operating points at a measurement interval of 1 second.

$$COP = \frac{\dot{Q}_{SI}}{P_{el}} = \frac{\dot{V}_{SI,in} \cdot \rho_{SI,in} \cdot (h_{SI,out} - h_{SI,in})}{P_{el}} \quad (3)$$

The power consumption of the heat pump is measured at the terminal of the frequency inverter with a wattmeter.

2.3. Experimental investigation of optimum high side pressure

In order to determine the influence of the high-side pressure on the COP the high-side pressure was varied while the heat sink and source temperatures, the suction gas superheat and the compressor speed were set constant. It was found that an optimum value for the high-side pressure exists. Fig. 3 shows t/h-diagrams of measured sub-critical operating points at a pressure lower than the optimum pressure, close to the optimum pressure and at a too high pressure from left to right. During sub-critical operation the location of the pinch point in the condenser is determined by the sink temperature levels and the condensing temperature. Through controlling the high-side pressure, the EXV determines the condensation temperature. At too low high-side pressures, as shown in Fig. 3 (left), the pinch point occurs at the refrigerants dew line, i.e. within the condenser. This limits the heat transfer leading to an increased refrigerant temperature at the condenser exit (state point 4) which reduces the heating capacity. Increasing the high-side pressure increases the compressor outlet temperature to the cost of increased compression work. Too high pressure levels as seen in Fig. 3 (right) decrease the COP since the pinch point at the condenser outlet limits the heat transfer and the increase in

heating capacity is outmatched by the increase in compression work. In between these two cases an optimum high-side pressure, as depicted in Fig. 3 (middle), yielding the maximum COP can be found.

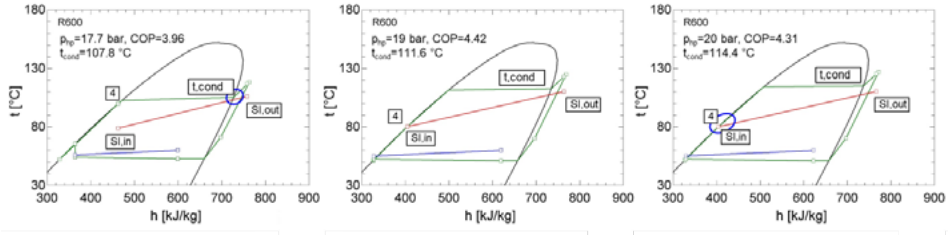

Fig. 3. t/h-diagrams of measured sub-critical operating points at different high-side pressures at source inlet/outlet temperatures of 60/55 °C, sink inlet/outlet temperatures of 80/110 °C and a suction gas superheat of $\Delta T_{sup,1}$=20 K

Similar observations can be made during trans-critical operation. At a constant compressor inlet state, the compressor outlet temperature and subsequently the condenser inlet temperature (state point 3) depend on the high-side pressure. The location of the pinch point in the condenser depends on the condenser inlet state, thus the heat transfer in the condenser is affected by the high-side pressure.

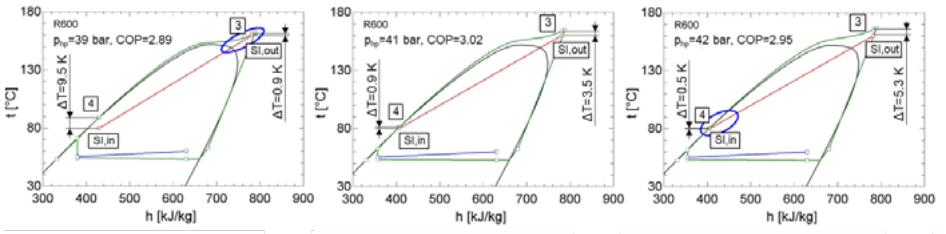

Fig. 4. t/h-diagrams of measured trans-critical operating points at different high-side pressures at source inlet/outlet temperatures of 60/55 °C, sink inlet/outlet temperature of 80/160 °C and a suction gas superheat of $\Delta T_{sup,1}$=10 K

The second operating parameter studied experimentally is the suction gas superheat. Fig. 5 shows the dependency of the COP on the high-side pressure for 10 K, 15 K and 20 K of suction gas superheat at the compressor inlet.

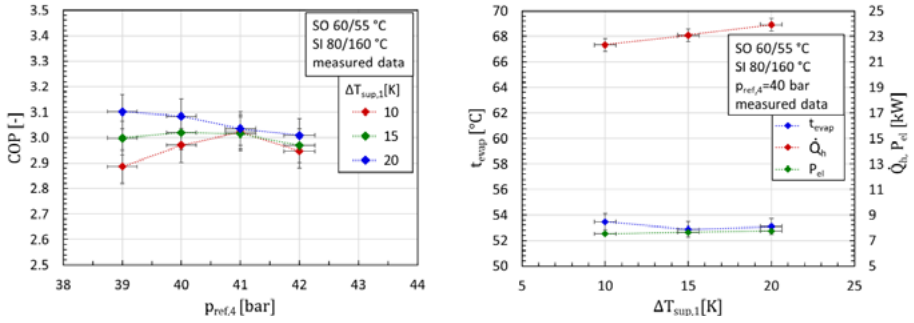

Fig. 5. Measured COP at source inlet/outlet temperatures 60/55 °C and sink inlet/outlet temperatures 80/160 °C for different values of suction gas superheat (left) and the influence of the superheat on evaporation temperature and capacities (right)

It can be seen that by increasing the suction gas superheat in the IHX the levels for optimum high-side pressure can be shifted to lower values while an increase of the COP is possible, which is in agreement with

the simulation study conducted by Verdnik et al [7]. This is possible because the increase in suction gas superheat established in the IHX does not lead to a drop in the evaporating temperature as can be seen in Fig. 5 (right). The increased condenser inlet temperature lead to an increase in the heating capacity which is larger than the increase in compressor power, which subsequently leads to the observed increase in the COP.

3. Simulation model

The TIL Suite package [10] was used to develop a simulation model of the trans-critical heat pump. This Dymola library contains models for components and media properties in the object-based Modelica language, Predefined models of the package have been modified or extended with user specific geometries or correlations for heat transfer and pressure drop.

3.1. Compressor model

The compressor is modeled using the overall isentropic efficiency, inner isentropic efficiency and volumetric efficiency according to equation (4), (5) and (6) respectively. The efficiencies are based on data extracted from the manufacturers' software [11]. As first experiments showed a stronger decline in the volumetric efficiency, the slope of the gained approximation was increased by 30 %. In order to calculate the power consumption at the terminal of the frequency inverter, an inverter efficiency of 95% is assumed according to equation (7), yet all simulations and measurements in this work have been conducted at an inverter frequency of 50 Hz.

$$\eta_{is,ov} = \frac{\dot{m}_{ref} \cdot (h_{ref,2s} - h_{ref,1})}{P_{comp}} = 0.684 - 0.002 \cdot \pi - 0.0004 \cdot \pi^2 \quad (4)$$

$$\eta_{is,i} = \frac{h_{ref,2s} - h_{ref,1}}{h_{ref,2} - h_{ref,1}} = 0.76 - 0.002 \cdot \pi - 0.0004 \cdot \pi^2 \quad (5)$$

$$\lambda_{vol} = \frac{\dot{m}_{ref}}{\rho_{ref,1} \cdot \dot{V}_{swept}} = 1.04 - 0.05 \cdot (1 + 30\%) \cdot \pi = 1.04 - 0.065 \cdot \pi \quad (6)$$

$$P_{el} = \frac{P_{comp}}{\eta_{FI}} = \frac{P_{comp}}{0.95} \quad (7)$$

3.2. Modelling of the heat exchangers

The TIL-Suite includes models for plate heat exchangers based on a finite volume approach. For the IHX and evaporator these models were used with a discretization of 10 cells. The model for the condenser was adopted to account for the asymmetric channel widths of the refrigerant and the water side and a discretization of 80 cells was used. A sinusoidal chevron pattern with an inclination angle of 60° was assumed for all heat exchangers. Table 3 shows the used geometry for the heat exchanger models as well as the correlations for the heat transfer coefficients (HTC) and pressure drops (Δp).

Table 3. Correlations used in the heat exchanger models

		Condenser		Evaporator	IHX		
		Refrigerant	Water				
Refrigerant	HTC	Forooghi and Hooman [12]		Longo [13]	Refrigerant	HTC	Forooghi and Hooman [12]
	Δp	Martin [14]		Longo [15]	high-pressure side	Δp	Martin [14]
Water	HTC	Martin [14]		Martin [14]	Refrigerant	HTC	Longo [13]
	Δp	Martin [14]		Martin [14]	low-pressure side	Δp	Martin [14]

3.3. Simulation study on variation of the operating parameters

The influence of suction gas superheat, heat source temperature level and heat sink inlet and outlet temperatures on the COP have been studied over a range of high-side pressures.

An increase of the suction gas superheat lowers the optimum high-side pressure and increases the COP as can be seen in Fig. 6. Since the heat sink inlet/outlet temperatures of 80/160 °C, as depicted in Fig. 6 (left), can be reached with pressures slightly above the critical pressure (37.96 bar), this effect can be seen clearer at sink inlet/outlet temperatures of 80/170 °C, as depicted in Fig. 6 (right).

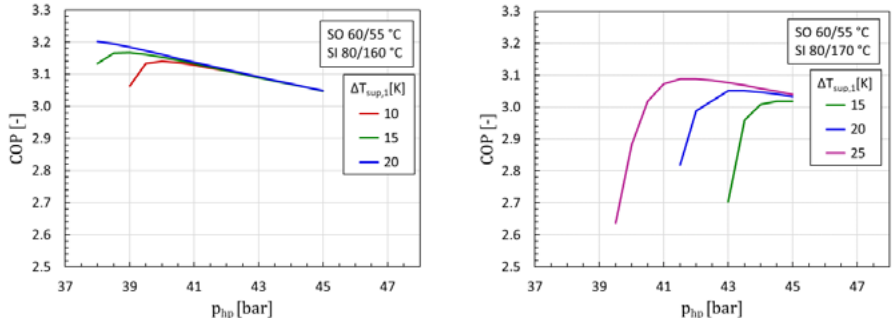

Fig. 6. Simulated COP for different high-side pressures at varying suction gas superheat for source inlet/outlet temperatures 60/55 °C, sink inlet/outlet temperatures 80/160 °C (left) and heat sink inlet/outlet temperatures 80/170 °C (right)

A variation of the sink inlet temperature, as depicted in Fig. 7 (left), shows that an increase of the sink inlet temperature leads to a decrease of the COP, but the value of the optimum high-side pressure is not influenced. Varying the sink outlet temperature, as illustrated in Fig. 7 (right), shows that higher high-side pressures are necessary to achieve higher sink outlet temperatures, which leads to a decrease of the maximum COP. By comparing the two graphs it can be seen, that the system COP is more sensitive in a change of sink inlet temperature than sink outlet temperature.

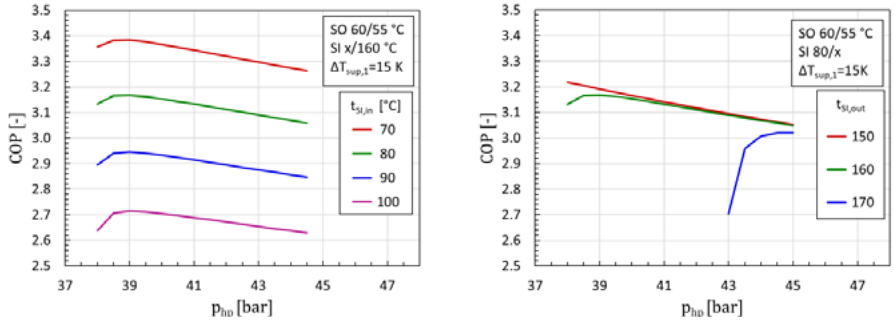

Fig. 7. Simulated COP for different high-side pressures at varying suction gas superheat for varying sink inlet temperature (left) and varying sink outlet temperature (right)

The last operating parameter to investigate is the heat source temperature. Fig. 8 shows a variation of the heat source temperature with a constant difference between inlet and outlet temperature of 5 K. As can be seen in Fig. 8 (left), an increase of the heat source temperature leads to an increase of the COP because of the reduced pressure ratio the compressor has to overcome. The level of the optimum high-side pressure is slightly shifted towards higher pressures but is very close to the minimum pressure needed to reach the set heat sink outlet temperature. As the heat source temperature determines the evaporation temperature, an increase of the heat source temperature leads to a strong increase in compressor power and heating capacity, as can be seen in Fig. 8 (right.)

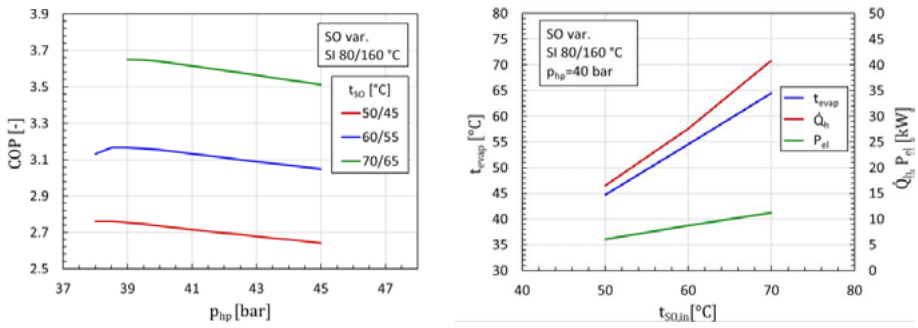

Fig. 8. COP for different high-side pressures at varying suction gas superheat at varying source temperatures (left) and the influence of the source temperature on evaporation temperature and capacities (right)

4. Simulation vs. measured data

Fig. 9 compares the results of the simulation model with the experimental data gathered with the prototype for the same operating point and different values of suction gas superheat. The simulation reflects the characteristic relation of the COP on the high-side pressure, although the value of the optimum high-side pressure is not exactly reproduced.

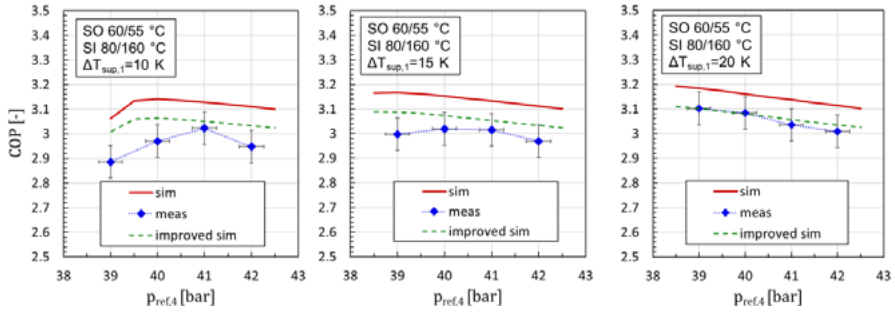

Fig. 9. Measured and simulated COP for heat source inlet/outlet temperatures 60/55 °C, heat sink inlet/outlet temperatures 80/160 °C and suction gas superheat of $\Delta T_{sup,1}$=10 K (left), 15 K (middle) and 20 K (right)

A direct comparison of the simulated and measured values for the COP, the heating capacity and the electric power consumption in Fig. 10 shows a deviation between simulation and experiment of +7%, +20% and +15% respectively which is caused by a slight overestimation of the evaporation temperature and compressor volumetric efficiency in the simulation. As first steps to improve the simulation model, the vapor quality at the accumulator outlet, the compressors volumetric efficiency, the pressure drop and assumptions regarding the plate pattern geometry in the evaporator were investigated. In the improved simulation model, the vapor quality at the outlet of the low-pressure accumulator was modelled with values less than unity depending on the filling level instead of the ideal behavior of saturated vapor. In the evaporator, momentum, manifold and port, and gravity pressure drop according to Longo et al. [13] were considered on the refrigerant side. The assumption regarding corrugation angle and pitch were altered to 10° and 10 times the corrugation height, respectively. The compressors volumetric efficiency was modelled with equation (8).

$$\lambda_{vol} = 0.945 - 0.056 \cdot \pi \tag{8}$$

The results of the improved simulation model yield a deviation to experimental data of less than 5% in COP, less than 7% for the heating capacity and less than 5% for the electric power consumption as can be seen in Fig. 10.

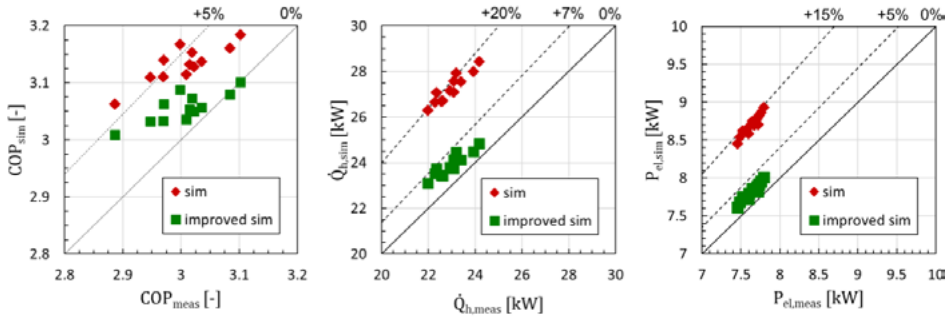

Fig. 10. Comparison of simulated and measured COP (left) heating capacity (middle) and electric power consumption (right)

5. Conclusions and Outlook

A prototype of a high-temperature vapor compression heat pump utilizing R600 in a one-stage cycle using a reciprocating compressor, low-pressure accumulator and IHX for suction gas superheating has been developed. First measurements prove the concept of using R600 in a trans-critical cycle. Tests conducted at heat source inlet/outlet temperatures of 60/55 °C showed a COP of 4.42 for heat sink inlet/outlet temperatures of 80/110 °C in sub-critical operation. Increasing the high-side pressure to values exceeding the critical pressure of the refrigerant enabled heat sink inlet/outlet temperatures of 80/160 °C, yielding a COP of up to 3.10 depending on the suction gas superheat and high-side pressure. Energy balances over the IHX showed that the refrigerant vapor quality at the outlet of the low-pressure accumulator is in the range of 0.9 depending on the operating point, which reduces the possible suction gas superheating in the IHX.

The originally introduced simulation model reproduced the system COP with a deviation of less than 7%, while the heating capacity and electric power consumption were overestimated by 20% and 15%, respectively. After further considerations regarding refrigerant vapor quality at the accumulator outlet, volumetric efficiency of the compressor and evaporator geometry and pressure drop, the deviation was reduced to less than 5%, 7% and 5% in COP, heating capacity and electric power consumption, respectively.

The next steps will be to conduct further measurements to evaluate the compressor and system efficiency as well as more detailed investigations regarding the refrigerant charge and pressure drop in the condenser. The simulation model will be refined and validated using experimental data. The operational envelope in terms of heat source temperatures, suction gas superheat and inverter frequency will be experimentally determined with respect to the compressor power and sufficient cooling of the electric motor. These insights should serve to develop a control strategy for the optimal high-side pressure and suction gas superheat depending on the operating conditions of the high-temperature heat pump.

Acknowledgements

This work has been conducted in the course of the cooperative project “TransCrit” (FFG No.: 865083) under the cooperation of Graz University of Technology and Frigopol Kälteanlagen GmbH. The project is funded by the Austrian Climate and Energy Fund and carried out within the Austrian Energy Research Program 2017.

References

[1] International Energy Agency. Energy Efficiency 2019. https://webstore.iea.org/market-report-series-energy-efficiency-2019 (4.11.2019).
[2] Lorentzen, G., 1990. Trans-critical vapour compression cycle device. Patent WO/07683.
[3] Besbes, K., Youghaib, A., De Carlan, F., Peureux, J.-L., 2015. A R-32 transcritical heat pump for high temperature industrial applications. 24th IIR Congress of Refrigeration, Yokohama, Japan, paper id: 599.
[4] Abi Chahla, G.; Beucher, Y., Zoughaib, A., De Carlan, F., Pierucci, J., 2019. Transcritical industrial heat pump using HFO’s for up to 150 °C hot air supply. 25th IIR Congress of Refrigeration, Montreal, Canada,

paper id: 1184.
[5] Kimura, T,, Fuchikami, H., Nishida, K., Kudo, M., Machida, A., Saito, K., Ohta, Y., Katsuta, M., 2018. Development of a high temperature heat pump using reusable heat as the heat source. JRAIA International Symposium 2018, Kobe, Japan.
[6] Verdnik, M., Rieberer, R., & Baumhakel, A. (2020). Entwicklung einer transkritischen R600-Hochtemperaturwärmepumpe. 45th Annual Meeting of the Deutscher Kaelte und Klimatechnischer Verein 2019: Deutsche Kaelte-und Klimatagung 2019 Ulm, Germany, pp. 1325-1334
[7] Verdnik, M., Rieberer, R., Moisi, H., 2019. Trans-critical vapor compression cycle using butane (R600) as refrigerant for industrial waste heat recovery. 25th IIR Congress of Refrigeration, Montréal, Canada, paper id: 1186.
[8] Moisi, H., Rieberer, R., 2017. Refrigerant Selection and Cycle Development for a High Temperature Vapor Compression Heat Pump. 12th IEA Heat Pump Conference 2017, Rotterdam, Netherlands, paper id: O.3.4.3.
[9] EES, 2019. Engineering Equation Solver v. 10.644, F-Chart Software, Madison, Wisconsin.
[10] TLK-Thermo, 2018. TIL Suite v.3.8.0, TLK-Thermo GmbH, Braunschweig, Germany
[11] Bitzer, 2018. Bitzer Software v. 6.9.2074, BITZER Kühlmaschinenbau GmbH, Sindelfingen, Germany.
[12] Forooghi, P., Hooman, K., 2014. Experimental analysis of heat transfer of supercritical fluids in plate heat exchangers. International Journal of Heat and Mass Transfer 74, p. 448-459
[13] Longo, G. A., Mancin, S., Righetti, G., Zilio, C., 2015. A new model for refrigerant boiling inside Brazed Plate Heat Exchangers (BPHEs). International Journal of Heat and Mass Transfer 91, p. 144–149.
[14] Martin, H., 2013. Druckverlust und Wärmeübergang in Plattenwärmeübertragern. Verein Deutscher Ingenieure, VDI-Wärmeatlas, Springer Vieweg, Berlin, p. 1687-1693
[15] Longo, G. A., 2012. Hydrocarbon Refrigerant Vaporization Inside a Brazed Plate Heat Exchanger. Journal of Heat Transfer (134).